State-of-the-art multi-reference EDF calculations.
I. Odd (and some other) Systems

Michael Bender

Institut de Physique Nucléaire de Lyon
CNRS/IN2P3 & Université de Lyon & Université Lyon 1
69622 Villeurbanne, France

Workshop on
"Symmetry-breaking versus symmetry-preserving schemes:
how to efficiently grasp collective correlations in mesoscopic many-body systems?"
ESNT, Saclay France

14th of May 2019

- **E**nergy **D**ensity **F**unctional: Expression for the energy given in terms of one-body density matrices (or local one-body densities).
- Instead of calculating the energy from an effective interaction, there is the (frequently used) possibility to postulate directly the form of the energy functional.
- **S**ingle-**R**eference EDF: Method where the EDF is calculated from the one-body density matrices of a variationally optimized single product state ("HF", "HFB").
- **M**ulti-**R**eference EDF: Method where the EDF is calculated from off-diagonal one-body density matrices $\rho^{LR}(x,x') \equiv \langle \mathrm{L} | \hat{a}^{\dagger}_{x'} \hat{a}_{x} | \mathrm{R} \rangle / \langle \mathrm{L} | \mathrm{R} \rangle$, covering the beyond-mean-field techniques "symmetry restoration" and "Generator Coordinate Method" in the EDF context (see lecture by L. Robledo)
- **pseudo-potential-based EDF**: EDF derived from a generating operator ("effective Hamiltonian")
- **pseudo-potential**: operator used to generate an EDF. Note: the notion of pseudo potential is also used for completely different concepts in quantum chemistry, nuclear physics, and other subfields of quantum physics.
- **Skyrme EDF**: Local energy density functional depending on local densities and currents containing gradients and simple density dependences.
- **Skyrme pseudo-potential**: momentum-dependent two-body + three-body + 4-body + ... pseudo-potential that is used as generator of the EDF.

particle-number projector

$$\hat{P}_{N_0} = \frac{1}{2\pi} \int_0^{2\pi} d\phi_N \underbrace{e^{-i\phi_N N_0}}_{\text{weight}} \overbrace{e^{i\phi_N \hat{N}}}^{\text{rotation in gauge space}}$$

angular-momentum restoration operator

$$\hat{P}^J_{MK} = \frac{2J+1}{16\pi^2} \int_0^{4\pi} d\alpha \int_0^{\pi} d\beta \, \sin(\beta) \int_0^{2\pi} d\gamma \, \underbrace{\mathcal{D}^{*J}_{MK}(\alpha, \beta, \gamma)}_{\text{Wigner rotation matrix}} \overbrace{\hat{R}(\alpha, \beta, \gamma)}^{\text{rotation in real space}}$$

K is the z component of angular momentum in the body-fixed frame.
Projected states are given by

$$|JMq\rangle = \sum_{K=-J}^{+J} f_J(K) \, \hat{P}^J_{MK} \, \hat{P}^Z \, \hat{P}^N \, |\mathrm{MF}(q)\rangle = \sum_{K=-J}^{+J} f_J(K) \, |JM(qK)\rangle$$

$f_J(K)$ is the weight of the component K and determined variationally

Axial symmetry (with the z axis as symmetry axis) allows to perform the α and γ integrations analytically, while the sum over K collapses, $f_J(K) \sim \delta_{K0}$

MR EDF: Configuration mixing by the symmetry-restored Generator Coordinate Method

Superposition of projected self-consistent mean-field states $|\text{MF}(\mathbf{q})\rangle$ differing in a set of collective and single-particle coordinates $\mathbf{q}$

$$|NZJM\nu\rangle = \sum_{\mathbf{q}} \sum_{K=-J}^{+J} f_{J,\kappa}^{NZ}(\mathbf{q},K)\, \hat{P}_{MK}^{J}\, \hat{P}^{Z}\, \hat{P}^{N}\, |\text{MF}(\mathbf{q})\rangle = \sum_{\mathbf{q}} \sum_{K=-J}^{+J} f_{J\nu}^{NZ}(\mathbf{q},K)\, |NZ\, JM(\mathbf{q}K)\rangle$$

with weights $f_{J\nu}^{NZ}(\mathbf{q},K)$.

$$\frac{\delta}{\delta f_{J\nu}^{*}(\mathbf{q},K)} \frac{\langle NZ\, JM\nu|\hat{H}|NZ\, JM\nu\rangle}{\langle NZ\, JM\nu|NZ\, JM\nu\rangle} = 0 \quad \Rightarrow \quad \text{Hill-Wheeler-Griffin equation}$$

$$\sum_{\mathbf{q}'} \sum_{K'=-J}^{+J} \left[\mathcal{H}_J^{NZ}(\mathbf{q}K,\mathbf{q}'K') - E_{J,\nu}^{NZ}\, \mathcal{I}_J^{NZ}(\mathbf{q}K,\mathbf{q}'K')\right] f_{J,\nu}^{NZ}(\mathbf{q}'K') = 0$$

with

$$\mathcal{H}_J(\mathbf{q}K,\mathbf{q}'K') = \langle NZ\, JM\, \mathbf{q}K|\hat{H}|NZ\, JM\, \mathbf{q}'K'\rangle \qquad \text{energy kernel}$$
$$\mathcal{I}_J(\mathbf{q}K,\mathbf{q}'K') = \langle NZ\, JM\, \mathbf{q}K|NZ\, JM\, \mathbf{q}'K'\rangle \qquad \text{norm kernel}$$

Angular-momentum projected GCM gives the

- correlated ground state for each value of J
- spectrum of excited states for each J

- In general, (non-normalised) projected matrix elements of an operator $\hat{T}$ read

$$\langle q|\hat{P}^{J}_{KM}\,\hat{T}\,\hat{P}^{J'}_{M'K'}|q'\rangle\,. \tag{1}$$

- If the operator is an irreducible tensor operator $\hat{T}^{\lambda}_{\mu}$, then the commutator $[\hat{T}^{\lambda}_{\mu}\,\hat{P}^{J'}_{M'K'}]$ is known from the general properties of the rotational group. For the special case of a scalar tensor operator $\hat{T}^{0}_{0}$ (i.e. a tensor operator of rank 0 like the Hamiltonian), one has $[\hat{T}^{0}_{0},\hat{P}^{J'}_{M'K'}]=0$.
- Using $\hat{P}^{J}_{KM}\hat{P}^{J'}_{M'K'}=\hat{P}^{J}_{KK'}\,\delta_{JJ'}\,\delta_{MM'}$, it follows that

$$\langle q|\hat{P}^{J}_{KM}\,\hat{T}^{0}_{0}\,\hat{P}^{J'}_{M'K'}|q'\rangle=\langle q|\hat{P}^{J}_{KK'}\,\hat{T}^{0}_{0}|q'\rangle\,\delta_{JJ'}\,\delta_{MM'}\,. \tag{2}$$

- It is sufficient to rotate one state to calculate matrix elements

$$\langle q|\hat{P}^{J}_{KK'}\,\hat{H}|q'\rangle=\frac{2J+1}{16\pi^2}\int_0^{4\pi}d\alpha\int_0^{\pi}d\beta\,\sin(\beta)\int_0^{2\pi}d\gamma\,\mathcal{D}^{*J}_{KK'}(\alpha,\beta,\gamma)\langle q|\hat{R}^{\dagger}(\alpha,\beta,\gamma)\hat{H}|q'\rangle\,. \tag{3}$$

Particle-number content

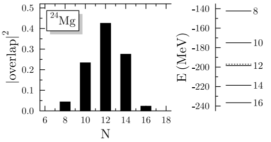

• "number parity" $\Rightarrow$ HFB state either decomposes into a state with only even or only odd particle number.

Angular-momentum content

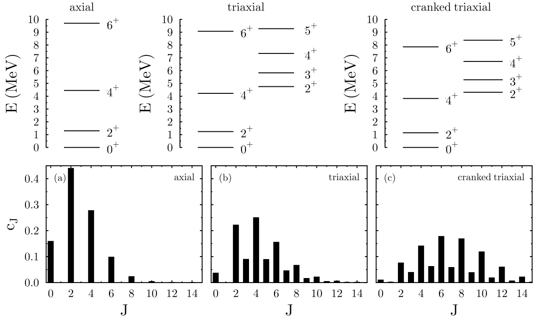

• Possible irreps and number of irreps with given J depend on intrinsic structure of symmetry-breaking state.

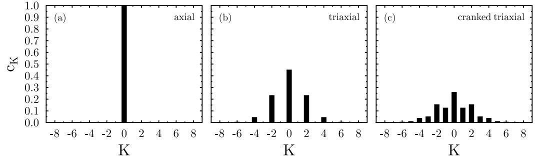

• Possible K components depend on orientation of state relative to z axis $\Rightarrow$ not unique.

- even-even nuclei
- BCS "ground states" with (mainly) axially-deformed reflection-symmetric shapes
- Skyrme EDF
- particle-number projection
- angular momentum projection
- mixing of different shapes
- Coordinate-space representation
- Lagrange mesh (which is a special case of DVR, which is equivalent to a disctretized plane-wave basis, where orthogonality of basis functions and partial integrations are numerically exact).

In Skyrme-EDF jargon, NLO means "next-to-leading order in gradients", i.e. the terms in the EDF contain zero (LO) or two (NLO) gradients. There are efforts to construct extended EDFs with four (N2LO) and six (N3LO) gradients. There is no reason to expect that this refers to a strict hierarchy in physical relevance, but it nevertheless refers a hierarchy in computational complexity.

$$\mathcal{E} = \mathcal{E}_{\text{kin}} + \mathcal{E}_{\text{Skyrme}} + \mathcal{E}_{\text{Coul}} + \mathcal{E}_{\text{pair}} + \mathcal{E}_{\text{corr}}$$

$$\begin{aligned}
\mathcal{E}_{\text{Skyrme}} = \int d^3r \sum_{t=0,1} \sum_{t_3=-t}^{+t} \Big\{ & C_t^{\rho\rho}[\rho_0]\rho_{tt_3}\,\rho_{t\,-t_3} + C_t^{\rho\tau}(\rho_{tt_3}\,\tau_{t\,-t_3} - \mathbf{j}_{tt_3}\cdot\mathbf{j}_{t\,-t_3}) \\
& + C_t^{\rho\Delta\rho}\rho_{tt_3}\Delta\rho_{t\,-t_3} + C_t^{ss}[\rho_0]\mathbf{s}_{tt_3}\cdot\mathbf{s}_{t\,-t_3} + C_t^{s\Delta s}\mathbf{s}_{tt_3}\cdot\Delta\mathbf{s}_{t\,-t_3} \\
& + C_t^{sT}\Big(\mathbf{s}_{tt_3}\cdot\mathbf{T}_{t\,-t_3} - \sum_{\mu,\nu=x,y,z}\mathbf{J}_{\mu\nu;tt_3}\mathbf{J}_{\mu\nu;t\,-t_3}\Big) \\
& + C_t^{\rho\nabla J}(\rho_{tt_3}\nabla\cdot\mathbf{J}_{t\,-t_3} + \mathbf{s}_{tt_3}\cdot\nabla\times\mathbf{j}_{t\,-t_3}) \\
& + C_t^{sF}\Big(\mathbf{s}_{tt_3}\cdot\mathbf{F}_{t\,-t_3} - \frac{1}{2}\sum_{\mu,\nu=x,y,z}\mathbf{J}_{\mu\nu;tt_3}\mathbf{J}_{\nu\mu;t\,-t_3} - \frac{1}{2}\sum_{\mu,\nu=x,y,z}\mathbf{J}_{\mu\mu;tt_3}\mathbf{J}_{\nu\nu;t\,-t_3}\Big) \\
& + C_t^{\nabla s\nabla s}(\nabla\cdot\mathbf{s}_{tt_3})(\nabla\cdot\mathbf{s}_{t-t_3}) \Big\}
\end{aligned}$$

$$
\begin{aligned}
\rho_q(\mathbf{r}) &= \rho_q(\mathbf{r},\mathbf{r}')\big|_{\mathbf{r}=\mathbf{r}'} \, , \\
\tau_q(\mathbf{r}) &= \nabla\cdot\nabla' \, \rho_q(\mathbf{r},\mathbf{r}')\big|_{\mathbf{r}=\mathbf{r}'} \, , \\
J_{q,\mu\nu}(\mathbf{r}) &= -\tfrac{i}{2}\left(\nabla_\mu - \nabla'_\mu\right) s_{q,\nu}(\mathbf{r},\mathbf{r}')\big|_{\mathbf{r}=\mathbf{r}'} \, , \\
\mathbf{s}_q(\mathbf{r}) &= \mathbf{s}_q(\mathbf{r},\mathbf{r}')\big|_{\mathbf{r}=\mathbf{r}'} \, , \\
\mathbf{T}_q(\mathbf{r}) &= \boldsymbol{\nabla}\cdot\boldsymbol{\nabla}' \, \mathbf{s}_q(\mathbf{r},\mathbf{r}')\big|_{\mathbf{r}=\mathbf{r}'} \, , \\
F_{q,\mu}(\mathbf{r}) &= \tfrac{1}{2}\sum_\nu \left(\nabla_\mu\cdot\nabla'_\nu + \nabla_\nu\cdot\nabla'_\mu\right) s_{q,\nu}(\mathbf{r},\mathbf{r}')\big|_{\mathbf{r}=\mathbf{r}'} \, , \\
\mathbf{j}_q(\mathbf{r}) &= -\tfrac{i}{2}\left(\nabla_\mu - \nabla'_\mu\right)\rho_q(\mathbf{r},\mathbf{r}')\big|_{\mathbf{r}=\mathbf{r}'} \, .
\end{aligned}
$$

Energy functional from a "density-dependent Skyrme force"

$$\mathcal{E}_{\text{Skyrme}} = \langle \text{HF} | \hat{t} + \hat{v}^{\text{central}} + \hat{v}^{\text{LS}} + \hat{v}^{\text{tensor}} | \text{HF} \rangle$$

- central

$$\begin{aligned}
\hat{v}^{\text{central}} \quad &= \quad t_0 \, (1 + x_0 \hat{P}_\sigma) \, \delta + \tfrac{1}{6} \, t_3 \, (1 + x_3 \hat{P}_\sigma) \, \rho^\alpha \, \delta \\
&\quad + \tfrac{1}{2} \, t_1 \, (1 + x_1 \hat{P}_\sigma) \big(\hat{\mathbf{k}}^{\dagger 2} \, \delta + \delta \, \hat{\mathbf{k}}^2 \big) \\
&\quad + t_2 \, (1 + x_2 \hat{P}_\sigma) \, \hat{\mathbf{k}}^\dagger \cdot \delta \, \hat{\mathbf{k}}
\end{aligned}$$

- spin-orbit

$$\hat{v}^{\text{LS}} \quad = \quad i W_0 \, (\hat{\boldsymbol{\sigma}}_1 + \hat{\boldsymbol{\sigma}}_2) \cdot \hat{\mathbf{k}}^\dagger \times \delta \, \hat{\mathbf{k}}$$

- tensor

$$\begin{aligned}
\hat{v}^{\text{tensor}} \quad &= \quad \tfrac{1}{2} t_e \left\{ \left[3 (\hat{\boldsymbol{\sigma}}_1 \cdot \hat{\mathbf{k}}^\dagger)(\hat{\boldsymbol{\sigma}}_2 \cdot \hat{\mathbf{k}}^\dagger) - (\hat{\boldsymbol{\sigma}}_1 \cdot \hat{\boldsymbol{\sigma}}_2) \, (\hat{\mathbf{k}}^\dagger)^2 \right] \delta + \text{h.c.} \right] \right\} \\
&\quad + \tfrac{1}{2} t_o \left\{ \left[3 (\hat{\boldsymbol{\sigma}}_1 \cdot \hat{\mathbf{k}}^\dagger) \, \delta \, (\hat{\boldsymbol{\sigma}}_2 \cdot \hat{\mathbf{k}}) + 3 (\hat{\boldsymbol{\sigma}}_2 \cdot \hat{\mathbf{k}}^\dagger) \, \delta \, (\hat{\boldsymbol{\sigma}}_1 \cdot \hat{\mathbf{k}}) - 2 (\hat{\boldsymbol{\sigma}}_1 \cdot \hat{\boldsymbol{\sigma}}_2) \, \hat{\mathbf{k}}^\dagger \cdot \hat{\mathbf{k}} \right] \right\}
\end{aligned}$$

- $\hat{\mathbf{k}} \equiv -\frac{i}{2}(\nabla_1 - \nabla_2)$, $\hat{P}_\sigma$: spin exchange operator
- Not all terms are always kept.
- Pairing energy is usually generated differently.
- Coulomb exchange is usually approximated, Coulomb pairing traditionally neglected.

Systematics of quadrupole correlation energies

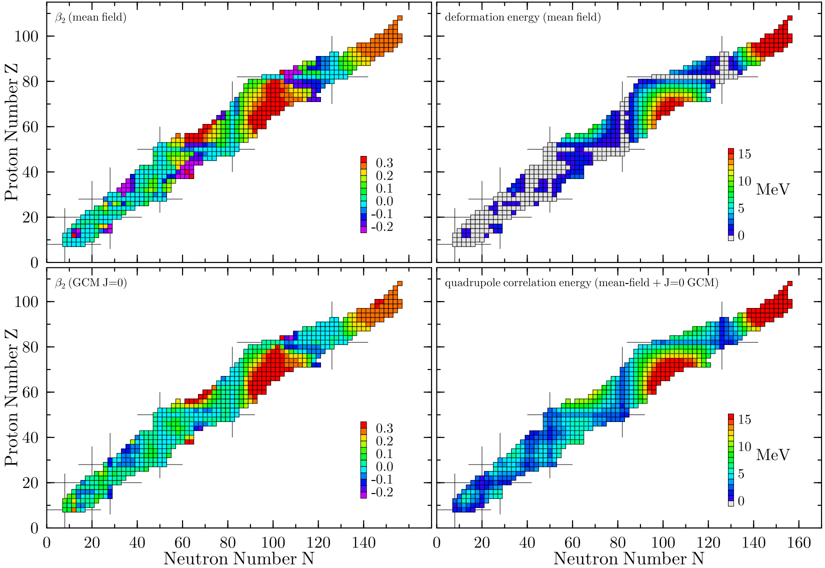

Bender, G. F. Bertsch, P.-H. Heenen, Phys. Rev. C 73 (2006) 034322

Systematics of quadrupole correlation energies

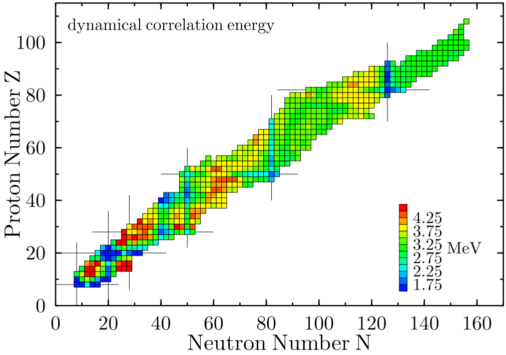

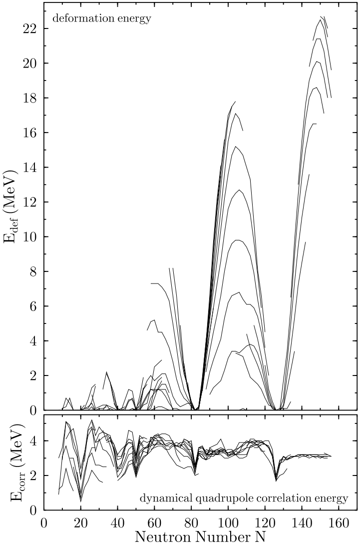

Bender, G. F. Bertsch, P.-H. Heenen, Phys. Rev. C 73 (2006) 034322

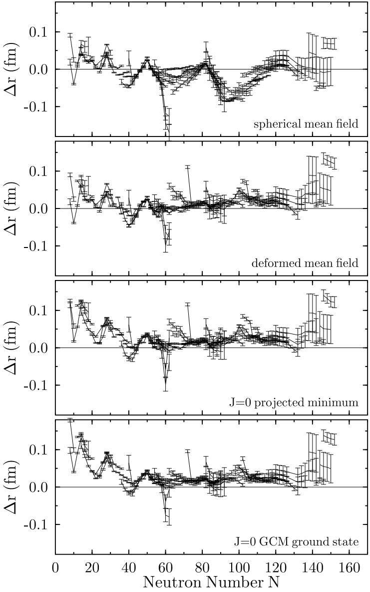

⇐ difference between calculated and experimental charge radius at four levels of modelling (from spherical mean field to symmetry-restored beyond-mean-field with shape fluctuations)

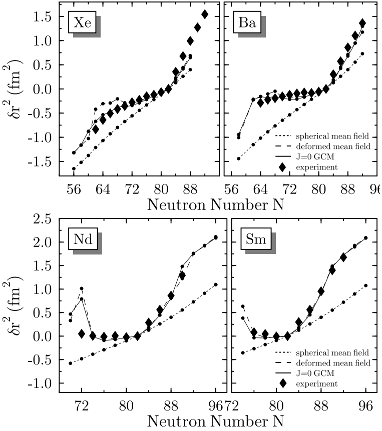

Bender, G. F. Bertsch and P.-H. Heenen, Phys. Rev. C 69 (2004) 034340

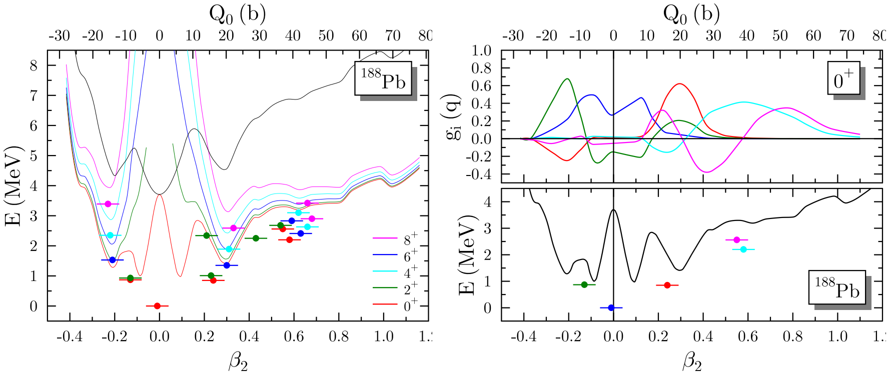

Bender, Bonche, Duguet, Heenen, PRC 69 (2004) 064303

Attention: $g_i^2(q)$ is not the probability to find a mean-field state with intrinsic deformation q in the collective state

for more complete systematics of Hg, Pb, Po isotopes see Yao, Bender, Heenen, PRC 87 (2013) 034322]

MR EDF is useful: Transition moments

Bender, Bonche, Duguet, Heenen, PRC 69 (2004) 064303.
Experiment: Grahn *et al*, PRL **97** (2006) 062501

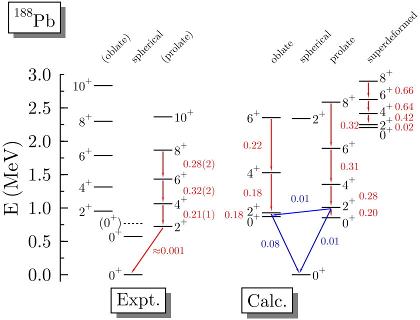

- in-band and out-of-band $E2$ transition moments directly in the laboratory frame with correct selection rules
- full model space of occupied particles
- only occupied single-particle states contribute to the kernels ("horizontal expansion")
- $\Rightarrow$ *no effective charges necessary*
- *no adjustable parameters*

$$B(E2; J'_{\nu'} \to J_\nu) = \frac{e^2}{2J'+1} \sum_{M=-J}^{+J} \sum_{M'=-J'}^{+J'} \sum_{\mu=-2}^{+2} |\langle J M \nu | \hat{Q}_{2\mu} | J' M' \nu' \rangle|^2$$

$$\beta_2^{(t)} = \frac{4\pi}{3R^2 A} \sqrt{\frac{B(E2; J \to J-2)}{(J\,0\,2\,0\,|(J-2)\,0)^2 e^2}} \quad \text{with} \quad R = 1.2\, A^{1/3}$$

Led to several collaborative projects on the interpretation of recent experimental data obtained in Jyväskylä (interpretation of excited states) and at ISOLDE (charge radii).

Horizontal vs. vertical expansion of correlations

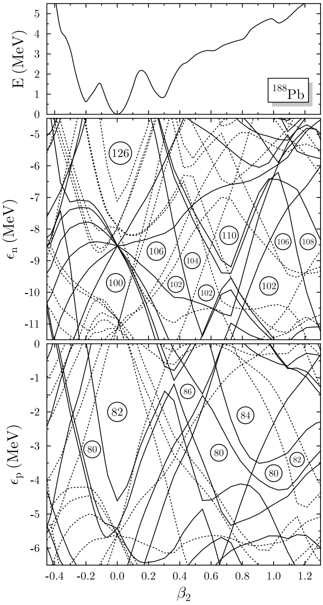

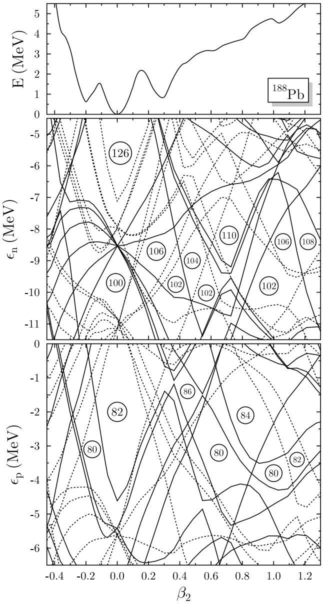

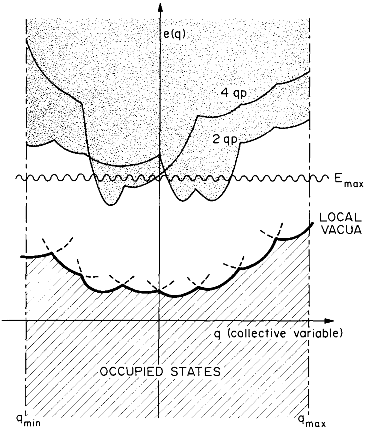

Fig. 1. Schematic plot of the energy versus the collective variable. The dark envelopes show the positions of the local vacua. The domain of the collective variable is defined by $q_{\min}$, $q_{\max}$ and the energy cut $E_{\max}$.

F. Dönau *et al*, NPA496 (1989) 333.

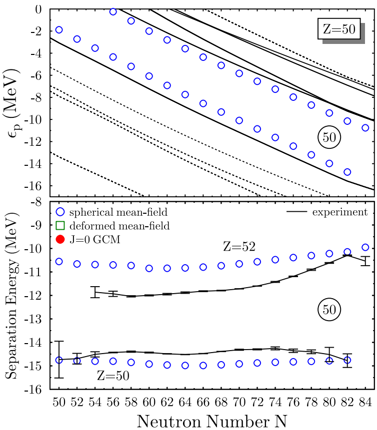

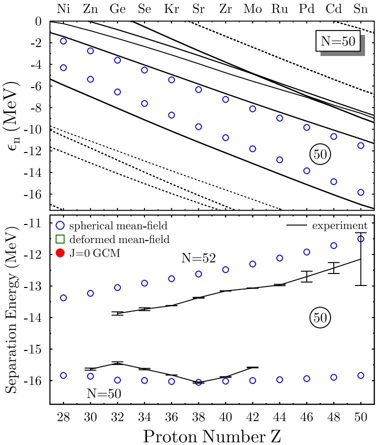

lower panel: $-S_{2p}(Z=50, N)/2$
The global linear trend is taken out subtracting
$\frac{N-82}{2}\,[S_{2p}(Z=50, N=50) - S_{2p}(Z=50, N=82)]$
using the spherical mean-field S_{2p} values

Bender, Bertsch, Heenen, PRC 78 (2008) 054312

lower panel: $-S_{2n}(Z, N=50)/2$
The global linear trend is taken out subtracting
$\frac{N-50}{2}\,[S_{2n}(Z=28, N=50) - S_{2n}(Z=50, N=50)]$
using the spherical mean-field S_{2n} values

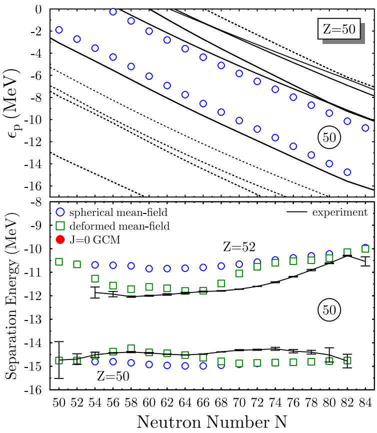

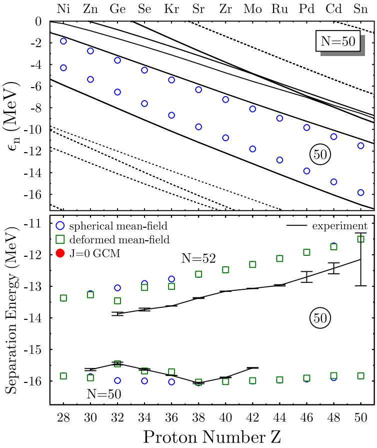

lower panel: $-S_{2p}(Z=50, N)/2$
The global linear trend is taken out subtracting
$\frac{N-82}{2}\,[S_{2p}(Z=50, N=50) - S_{2p}(Z=50, N=82)]$
using the spherical mean-field S_{2p}

Bender, Bertsch, Heenen, PRC 78 (2008) 054312

lower panel: $-S_{2n}(Z, N=50)/2$
The global linear trend is taken out subtracting
$\frac{N-50}{2}\,[S_{2n}(Z=28, N=50) - S_{2n}(Z=50, N=50)]$
using the spherical mean-field S_{2n}

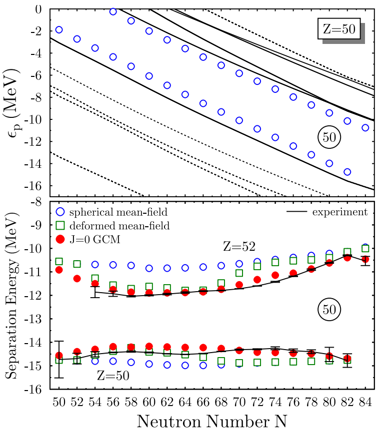

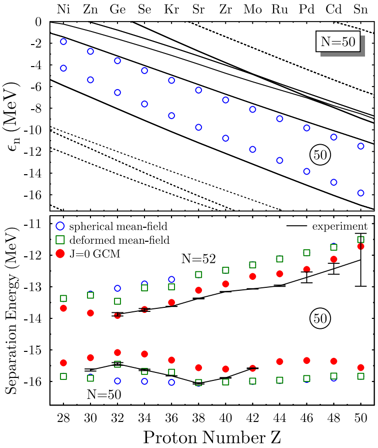

lower panel: $-S_{2p}(Z=50, N)/2$
The global linear trend is taken out subtracting
$\frac{N-82}{2}\,[S_{2p}(Z=50, N=50) - S_{2p}(Z=50, N=82)]$
using the spherical mean-field S_{2p}

lower panel: $-S_{2n}(Z, N=50)/2$
The global linear trend is taken out subtracting
$\frac{N-50}{2}\,[S_{2n}(Z=28, N=50) - S_{2n}(Z=50, N=50)]$
using the spherical mean-field S_{2n}

Bender, Bertsch, Heenen, PRC 78 (2008) 054312

MR EDF is useful: (non-) evolution of shells

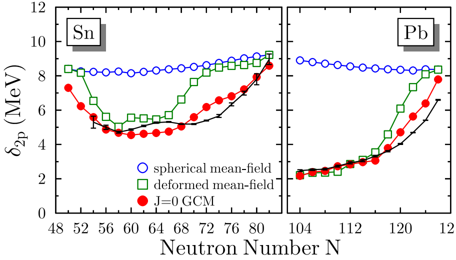

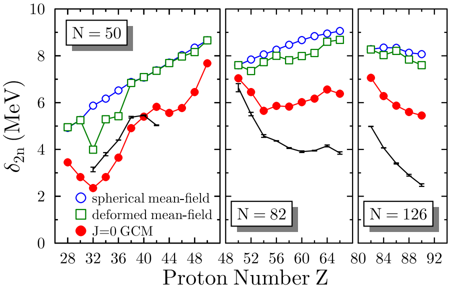

- In spite of their name, two-nucleon gaps $\delta_{2q}(N,Z)$ do not measure the gap in the single-particle spectrum in a self-consistent mean-field model

  Bender, Bertsch, Heenen, PRL 94 (2005) 102505
  Bender, Bertsch, Heenen, PRC 73 (2006) 034322
  experimental values shown here include more recent data than the plots in the papers

  For a pure mean-field analysis see also Bender, Cornelius, Lalazissis, Maruhn, Nazarewicz, and Reinhard, EPJ A14 (2002) 23

- see also the concept of "mutually enhanced magicity" discussed in Schmidt *et al*, NPA 318 (1979) 253; Zeldes, Dumitrescu, Köhler, NPA 399 (1983) 11]
- However, recall that the (non-observable) internal mechanism causing the evolution of the $\delta_{2q}(N,Z)$ is quite different (by construction) in valence-space CI and EDF methods.

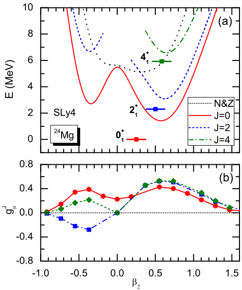

J. M. Yao, Bender, P.-H. Heenen, PRC 91 (2015) 024301

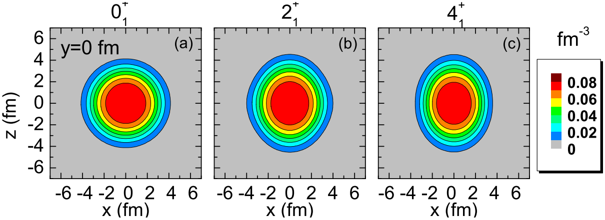

Contour plots of the 3D proton densities (in fm^{-3}) in the $y = 0$ plane for the 0^+_1 (a), 2^+_1, $M = 0$ (b), 4^+_1, $M = 0$ (c) states of ^{24}Mg.

Transition density in the laboratory between GCM states $|J_i M_i \mu_i\rangle$ and $|J_f M_f \mu_f\rangle$ assuming axial HFB states

$$\rho^{J_f M_f \mu_f}_{J_i M_i \mu_i}(\mathbf{r}) = \sum_{q_f, q_i} f^{J_f *}_{\mu_f, q'} \langle q' | \hat{P}^{J_f}_{0M_f} \, \hat{\rho}(\mathbf{r}) \, \hat{P}^{J_i \dagger}_{0M_i} \, \hat{P}^N \, \hat{P}^Z | q \rangle \, f^{J_i 0}_{\mu_i, q}$$

with

$$\langle q' | \hat{P}^{J_f}_{0M_f} \, \hat{\rho}(\mathbf{r}) \, \hat{P}^{J_i \dagger}_{0M_i} \, \hat{P}^N \, \hat{P}^Z | q \rangle$$

$$= \frac{\hat{J}_i^2 \, \hat{J}_f^2}{(8\pi^2)^2} \int d\Omega' \, D^{J_f *}_{0M_f}(\Omega') \sum_K D^{J_i}_{K0}(\Omega') \int d\Omega'' \, D^{J_i}_{0K}(\Omega'') \langle q' | \hat{\rho}(\tilde{\mathbf{r}}_{\Omega'}) \, \hat{P}^N \, \hat{P}^Z \, \hat{R}^\dagger(\Omega'') | q \rangle$$

$$\equiv \frac{\hat{J}_f^2}{8\pi^2} \int d\Omega' \, D^{J_f *}_{0M_f}(\Omega') \sum_K D^{J_i}_{KM_i}(\Omega') \, \hat{R}^\dagger(\Omega') \, \rho^{J_f J_i K 0}_{q' q}(\mathbf{r})$$

For the density of the GCM state $|JM\mu\rangle$ one obtains

$$\rho^{JM\mu}_{JM\mu}(\mathbf{r}) = \sum_{q_f, q_i} f^{J*}_{\mu, q'} \, f^{J0}_{\mu, q} \sum_\lambda Y_{\lambda 0}(\hat{\mathbf{r}}) \, \langle JM\lambda 0 | JM \rangle \sum_K \langle J0\lambda K | JK \rangle \int \mathrm{d}\hat{\mathbf{r}}' \, \rho^{JJK0}_{q' q}(r, \hat{\mathbf{r}}') \, Y^*_{\lambda K}(\hat{\mathbf{r}}')$$

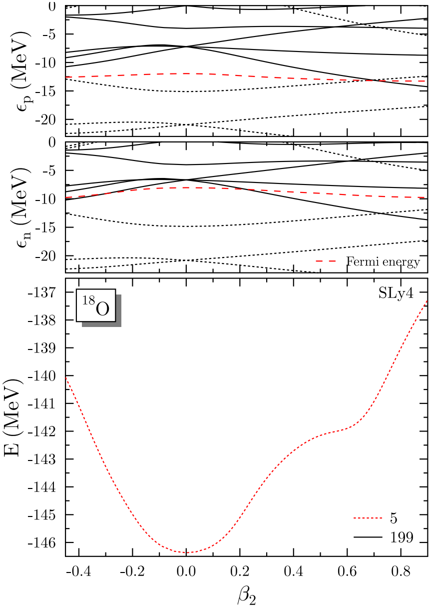

- pure particle-number projection

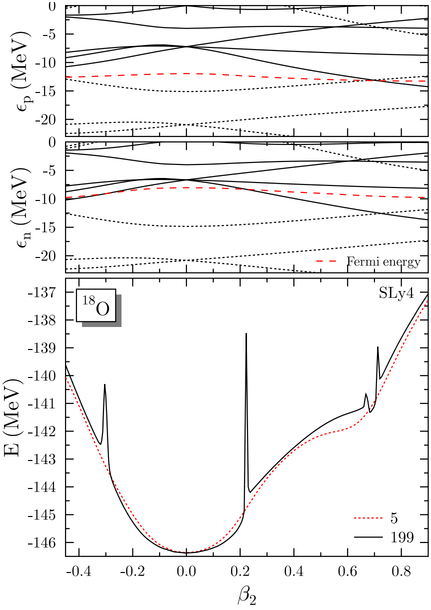

- pure particle-number projection
- first hints from Hamiltonian-based approaches: Dönau, PRC 58 (1998) 872; Almehed, Frauendorf, Dönau, PRC 63 (2001) 044311; Anguiano, Egido, Robledo NPA696 (2001) 467
- First analysis in a strict energy density functional (EDF) framework and of EDF-specific consequences by Dobaczewski, Stoitsov, Nazarewicz, Reinhard, PRC 76 (2007) 054315
- Further analysis of the EDF case by Lacroix, Duguet, Bender, PRC 79 (2009) 044318; Bender, Duguet, Lacroix, PRC 79 (2009) 044319; Duguet, Bender, Bennaceur, Lacroix, Lesinski, PRC 79 (2009) 044320; Bender, Avez, Duguet, Heenen, Lacroix, *in preparation*
- A different manifestation of the same problem is discussed by Tajima, Flocard, Bonche, Dobaczewski and Heenen, NPA542 (1992) 355 for EDF kernels between HFB vacua and two-quasiparticle states.
- More on that in the second talk I have been asked to give this week. Stay tuned.
- Use true Hamiltonian for further calculations.

Minimal form: SLyMR0

$$
\begin{aligned}
\hat{v} = {} & t_0 \left(1 + x_0 \hat{P}_\sigma\right) \hat{\delta}_{r_1 r_2} \\
& + \frac{t_1}{2} \left(1 + x_1 \hat{P}_\sigma\right) \left(\hat{\mathbf{k}}_{12}'^{2} \hat{\delta}_{r_1 r_2} + \hat{\delta}_{r_1 r_2} \hat{\mathbf{k}}_{12}^{2}\right) \\
& + t_2 \left(1 + x_2 \hat{P}_\sigma\right) \hat{\mathbf{k}}_{12}' \cdot \hat{\delta}_{r_1 r_2} \hat{\mathbf{k}}_{12} \\
& + \mathrm{i}\, W_0 \left(\hat{\boldsymbol{\sigma}}_1 + \hat{\boldsymbol{\sigma}}_2\right) \cdot \hat{\mathbf{k}}_{12}' \times \hat{\delta}_{r_1 r_2} \hat{\mathbf{k}}_{12} \\
& + u_0 \left(\hat{\delta}_{r_1 r_3} \hat{\delta}_{r_2 r_3} + \hat{\delta}_{r_3 r_2} \hat{\delta}_{r_1 r_2} + \hat{\delta}_{r_2 r_1} \hat{\delta}_{r_3 r_1}\right) \\
& + v_0 \left(\hat{\delta}_{r_1 r_3} \hat{\delta}_{r_2 r_3} \hat{\delta}_{r_3 r_4} + \hat{\delta}_{r_1 r_2} \hat{\delta}_{r_3 r_2} \hat{\delta}_{r_2 r_4} + \cdots\right)
\end{aligned}
$$

Sadoudi, Bender, Bennaceur, Davesne, Jodon, and Duguet, Physica Scripta T154 (2013) 014013

Pseudo-potentials for MR EDF. First try: SLyMR0

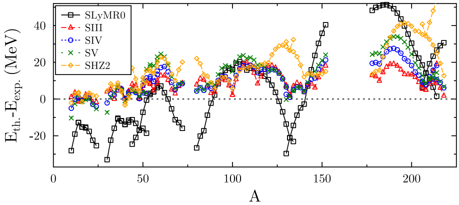

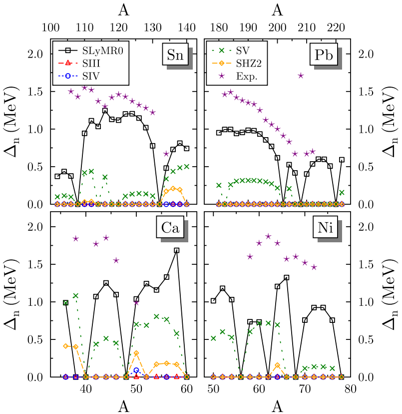

- it is impossible to fulfill the usual nuclear matter constraints , to have stable interactions and attractive pairing
- no "best fit" possible
- very bad performance compared to standard general functionals

Sadoudi, Bender, Bennaceur, Davesne, Jodon, and Duguet, Physica Scripta T154 (2013) 014013

- States in odd-A nuclei are described by 1qp- (or 3-qp, ..., $(2n-1)$-qp) excitations of a quasiparticle vacuum that describes an even nucleus

$$\beta_k^\dagger|\Phi\rangle$$

- Self-consistently determined product states describing odd-A nuclei always break symmetries.
- there are usually several possible low-lying states $\beta^\dagger|\Phi\rangle$ at each deformation
- Even when parity is conserved, blocked qp states can have either positive or negative parity.
- For each blocked orbital one can construct two different 1qp states, depending which of the two Kramers-degenerate level is blocked. When signature is a good quantum number, the projected states obtained from the two are the same, such that it is sufficient to block one.

States with same J^π, but different K mix:

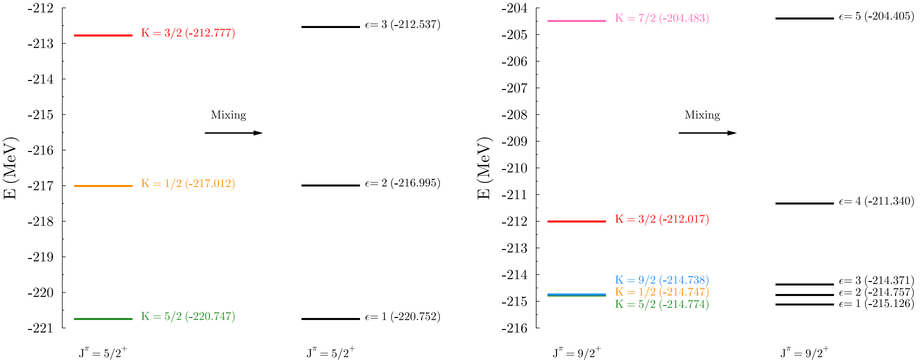

Bally, Avez, Bender, Heenen, unpublished

Different qp states mix

- (a) and (b) are the projected spectra from two different blocked 1qp states constrained to the same (triaxial) quadrupole deformation.
- (c) is the spectrum obtained by mixing the two sets of states.

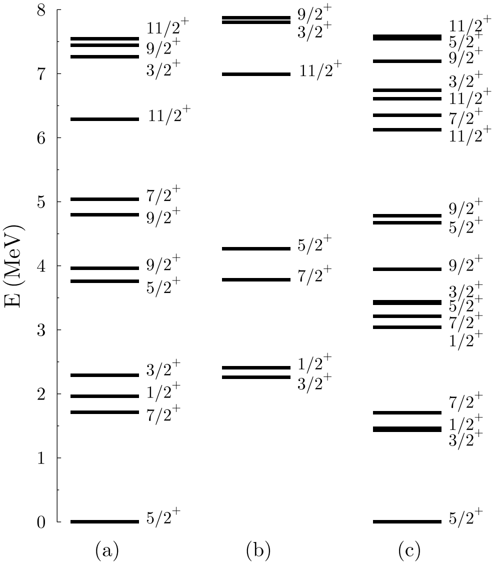

B. Bally, doctoral thesis, Université de Bordeaux (2014)

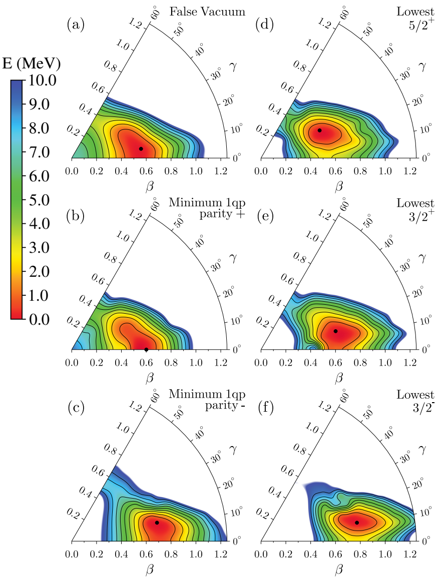

Angular-momentum and particle-number projected GCM of blocked triaxial one-quasiparticle states

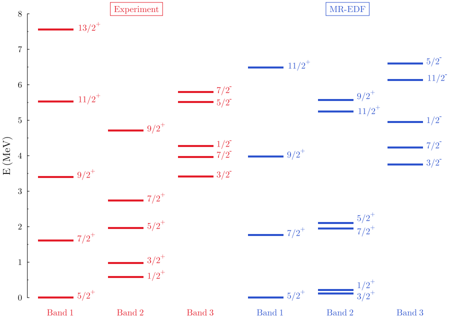

B. Bally, doctoral thesis, Université de Bordeaux (2014)

Proof-of-principle: Symmetry-restored GCM for ^{25}Mg

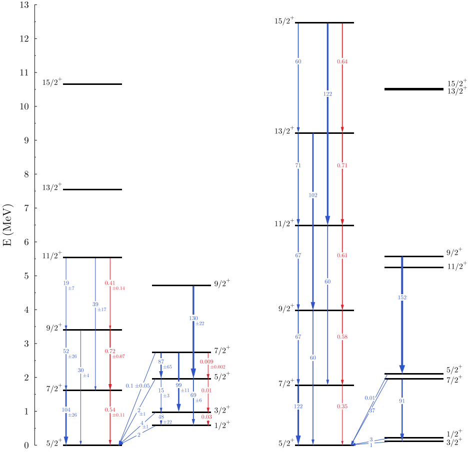

- spectroscopic quadrupole moment Q_s of the $5/2^+$ ground state:
  Exp: 20.1 ± 0.3 e fm^2
  Calc: 23.25 e fm^2
- magnetic moment μ of the $5/2^+$ ground state in nuclear magnetons:
  Exp: -0.855
  Calc: -1.054

Bally, Avez, Bender, Heenen, PRL 113 (2014) 162501

Data from Nuclear Data Sheets 110 (2009) 1691

Cranking: constructing HFB vacua with an auxiliary condition on the angular momentum $I = \rangle \Phi | \hat{J}_z | \Phi \rangle$

- Decomposition changes when cranking up a 1p state
- For cranked states, the two partner states decompose differently

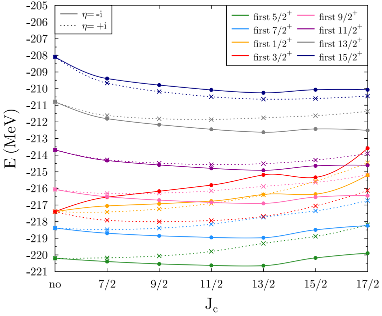

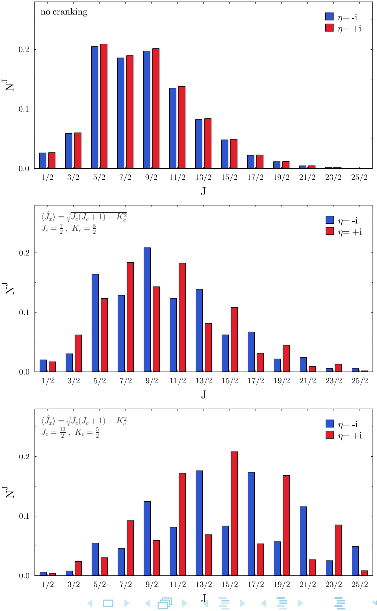

B. Bally, doctoral thesis, Université de Bordeaux (2014)

Low-lying states in ^{46}Ca

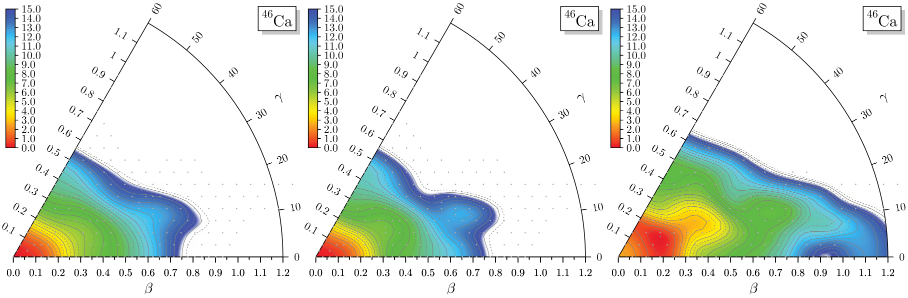

Left: Non-projected total energy of the HFB vacua (without LN correction) relative to the spherical configuration. Middle: $N = 26$, $Z = 20$ projected total energy of the HFB vacua relative to the spherical configuration. Right: Energy of the projected $N = 26$, $Z = 20$, $J = 0$ HFB vacua.

Bender, Bally, Heenen, to be published

Low-lying states in ^{46}Ca

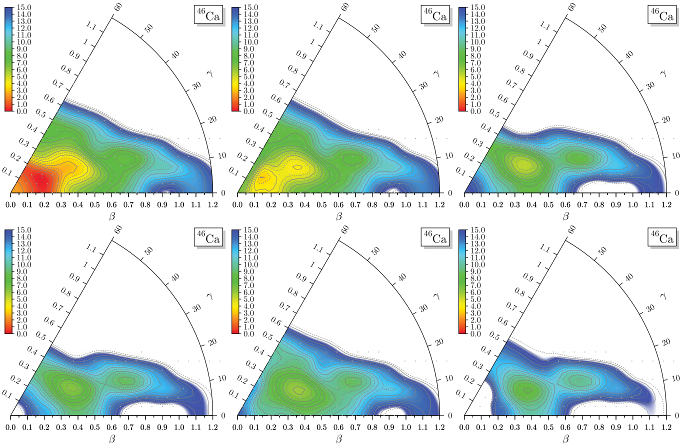

Top row: Right: Energy of the $J = 0$ HFB vacua. Middle: Energy of the lowest K-mixed $J = 2$ projected state . Right: Energy of the second K-mixed $J = 2$ state . Bottom row: Right: Energy of the $J = 3$ state. Middle: Energy of the lowest K-mixed $J = 4$ projected state. Right: Energy of the second K-mixed $J = 4$ state. The total energy is relative to the minimum of the $J = 0$ energy surface. All states are projected on $N = 26$, $Z = 20$,

Bender, Bally, Heenen, to be published

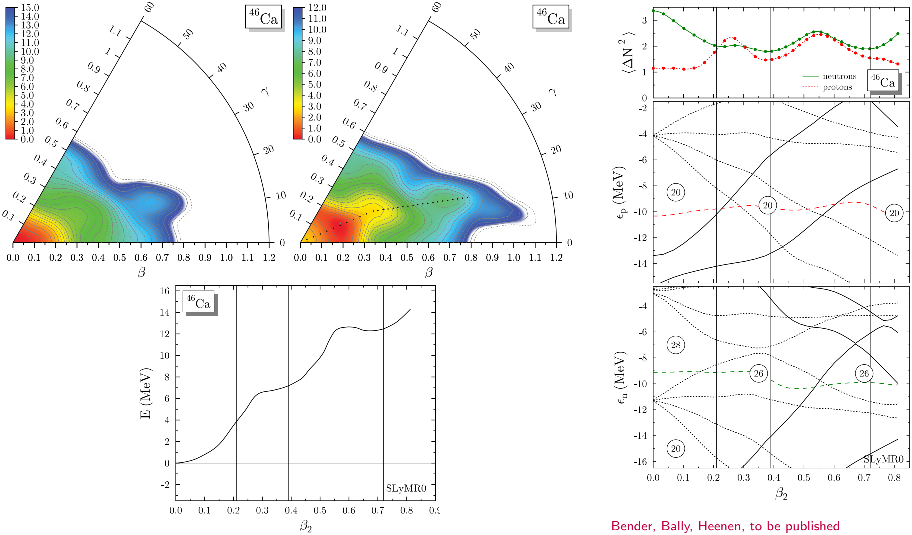

Bender, Bally, Heenen, to be published

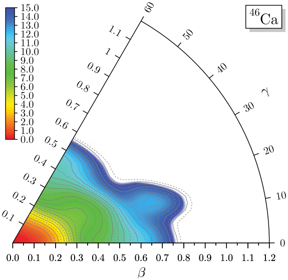

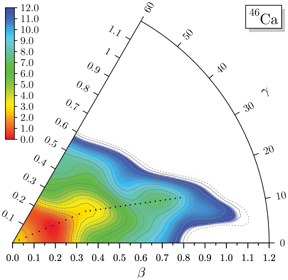

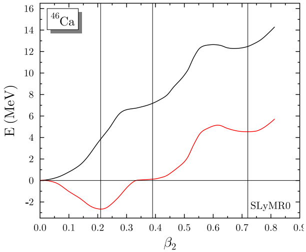

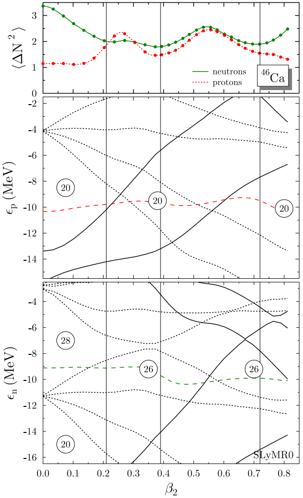

Bender, Bally, Heenen, to be published

Low-lying states in ^{46}Ca

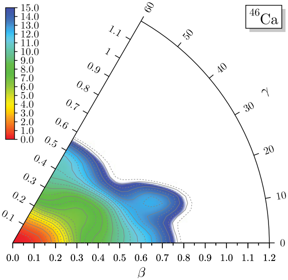

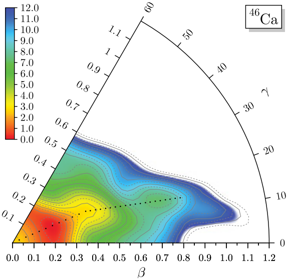

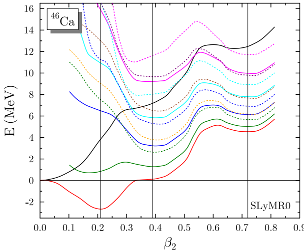

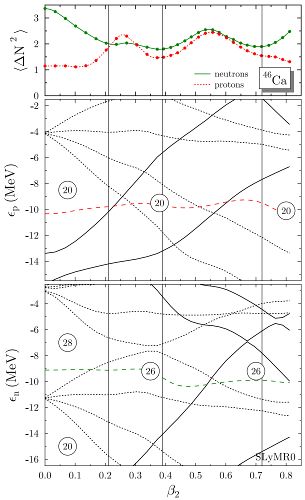

Bender, Bally, Heenen, to be published

Low-lying states in ^{46}Ca

collective wave function of the four lowest 0^+ states

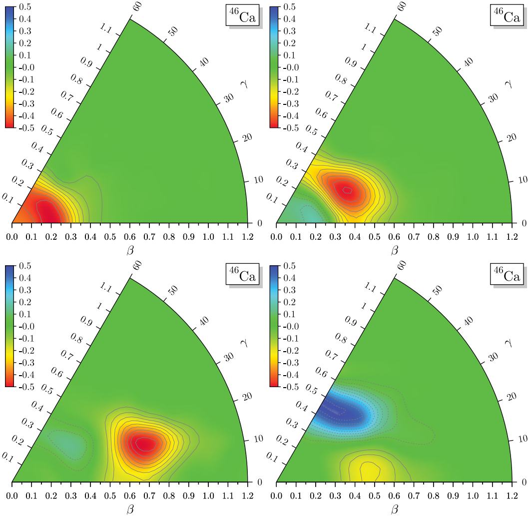

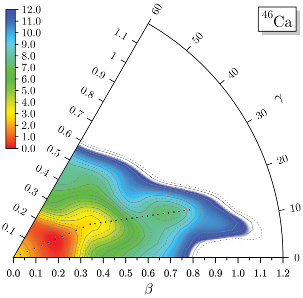

Bender, Bally, Heenen, to be published

Low-lying states in ^{46}Ca

collective wave function of the four lowest 0^+ states

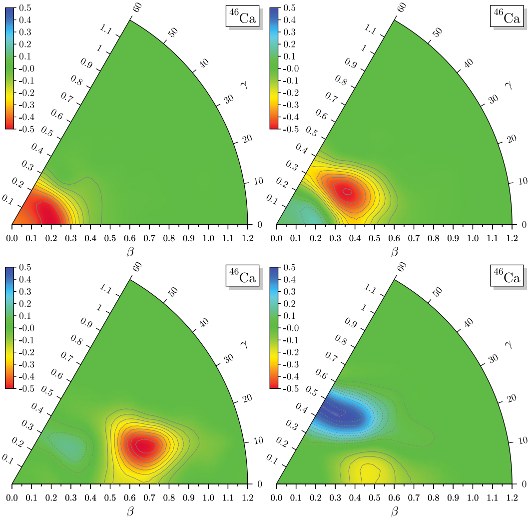

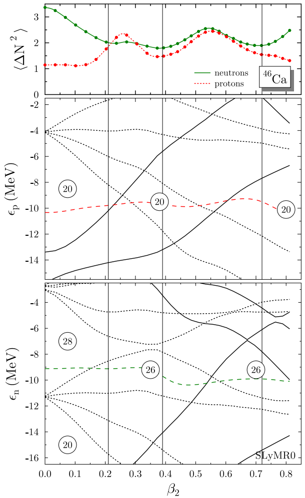

Bender, Bally, Heenen, to be published

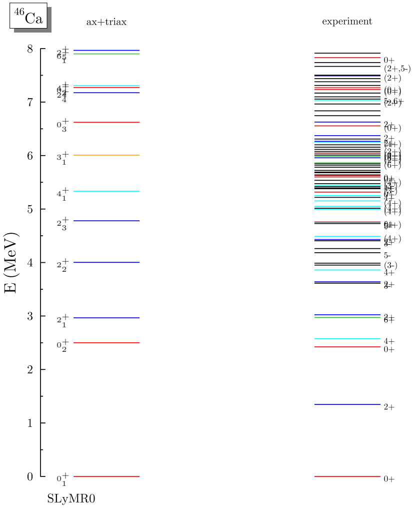

Bender, Bally, Heenen, to be published

- There is a sequence of "seniority-2" states with $J^\pi = 2^+$, 4^+, 6^+ that in the shell-model is easily obtained by coupling two neutron holes in the $1f_{7/2}$–shell to these angular momenta.
- These are non-collective; hence, cannot be described by "traditional" GCM.

Low-lying states in ^{46}Ca

seniority 0

N, Z, $J = 0$ projected

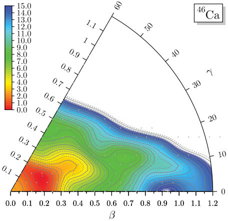

N, Z, $J = 6$ projected

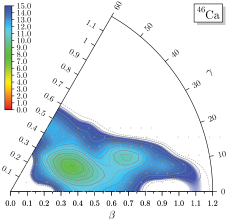

seniority 2, lowest N, Z, $J = 6$ projected

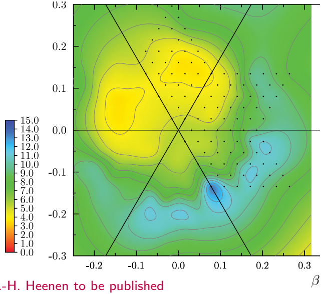

Bender& P.-H. Heenen to be published

seniority 0

N, Z, $J = 0$ projected

N, Z, $J = 6$ projected

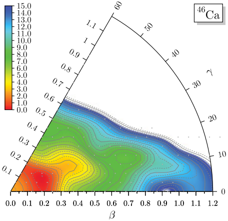

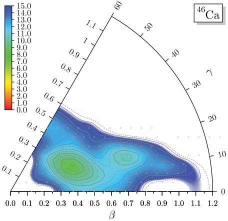

seniority 2, lowest N, Z, $J = 6$ projected

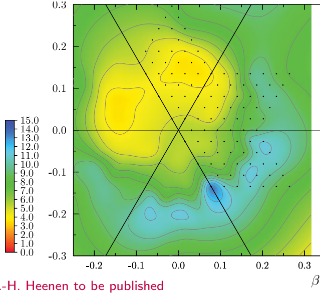

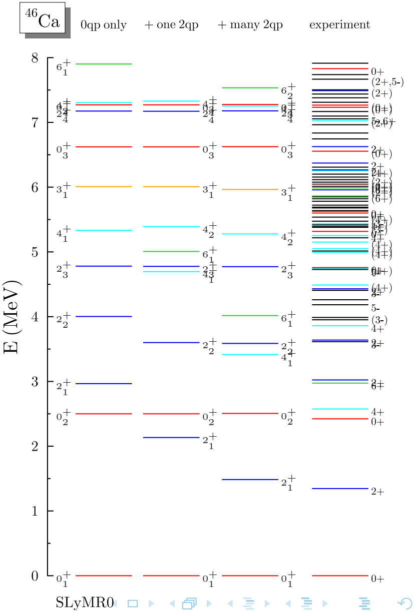

Bender& P.-H. Heenen to be published

collective wave function of the four lowest 0^+ states

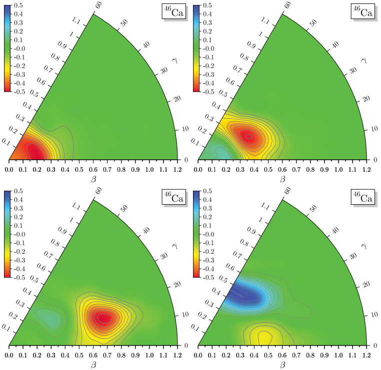

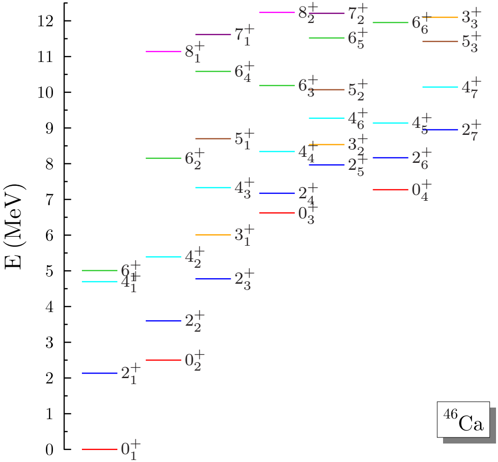

Bender, Bally, Heenen, to be published

Some preliminary results obtained with SLyMR1: ^{22,23,24,25,26,28}Ca

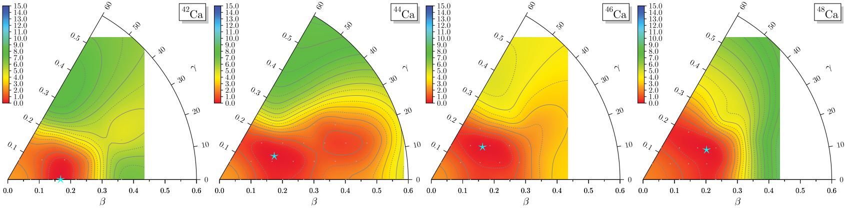

- Particle-number and $J = 0$ projected energy surfaces obtained with SLyMR1
- Ground state of ^{44}Ca is at a deformation where neutron pairing correlations vanish and proton pairing sets in.
- The more deformed minimum gives the lowest $J = 2$ projected energy of ^{44}Ca ...

N	HFB(sph)	HFB(def)	PNZ(sph)	PNZ(def)	PNZJ
22	-358.802	-358.843	-358.639	-358.764	-361.354
23	-367.054	-367.054	-367.098	-367.098	-368.460
24	-377.155	-377.244	-376.943	-377.190	-379.551
25	-385.657	-385.708	-385.522	-385.679	-387.823
26	-396.066	-396.085	-395.917	-396.134	-398.416

	N	HFB(sph)	HFB(def)	PNZ(sph)	PNZ(def)	PNZJ	experiment
	23	0.925	0.990	0.693	0.879	1.993	1.599
3-point gaps	24	0.799	0.863	0.633	0.801	1.410	1.858
	25	0.954	0.956	0.908	0.983	1.161	1.490

	N	HFB(sph)	HFB(def)	PNZ(sph)	PNZ(def)	PNZJ	experiment
5-point gap	24	0.869	0.918	0.717	0.866	1.493	1.701

Bender *et al*, unpublished

Proof-of-principle: Symmetry-restoration for ^{251}Md

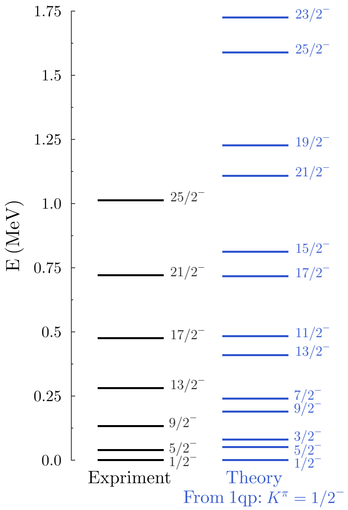

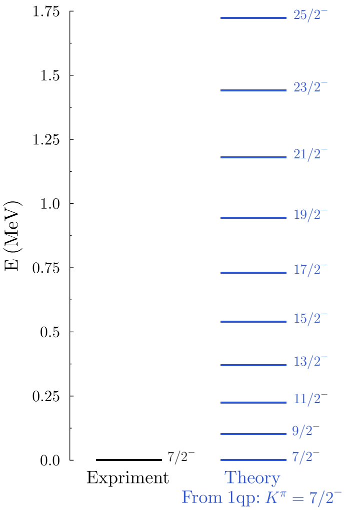

Bally, Bender, Heenen, unpublished

Other observables:

- radii
- magnetic moments μ
- spectroscopic quadrupole moments Q_s
- $B(E2)$ values
- $B(M1)$ values

J	rrmsp (fm)	rrmsn (fm)	mu (mu_N)	Q_s e fm^2	<Lz>	<Sz>	<Jz>	J
7/2	5.8769	6.0193	1.4540	596.84	3.835	-0.335	3.500	3.501
9/2	5.8769	6.0194	1.8407	232.67	4.753	-0.253	4.500	4.500
11/2	5.8769	6.0194	2.2308	14.27	5.692	-0.192	5.500	5.500
13/2	5.8769	6.0194	2.6230	-127.63	6.644	-0.144	6.500	6.500
15/2	5.8770	6.0194	3.0164	-225.40	7.604	-0.104	7.500	7.500
17/2	5.8770	6.0195	3.4108	-295.86	8.570	-0.069	8.500	8.500
19/2	5.8771	6.0195	3.8057	-348.48	9.539	-0.039	9.500	9.500
21/2	5.8771	6.0196	4.2011	-388.91	10.512	-0.012	10.500	10.500
23/2	5.8772	6.0196	4.5968	-420.74	11.487	0.013	11.501	11.500
25/2	5.8773	6.0197	4.9928	-446.29	12.464	0.037	12.501	12.500

transition	B(E2) (e^2 fm^4)	M(M1) (mu_N^2)
9/2 -> 7/2	55214	2.6167 E-04
11/2 -> 7/2	11834	---
11/2 -> 9/2	55760	3.9979 E-04
13/2 -> 9/2	21953	---
13/2 -> 11/2	47809	4.8087 E-04

- Results from MR EDF calculations are useful and instructive is many respects.

The work presented here would have been impossible without my collaborators

founding fathers

Paul Bonche	SPhT, CEA Saclay
Hubert Flocard	CSNSM Orsay
Paul-Henri Heenen	Université Libre de Bruxelles

formal aspects of the big picture

Thomas Duguet	Irfu/CEA Saclay & KU Leuven & NSCL/MSU
Denis Lacroix	IPN Orsay

design and implementation of code extensions

Benoît Avez	CEN Bordeaux Gradignan
Benjamin Bally	CEN Bordeaux Gradignan, now UNC Chapel Hilly
Veerle Hellemans	Université Libre de Bruxelles
Jiangming Yao	Université Libre de Bruxelles
Wouter Ryssens	IPN Lyon, now Yale University

development and benchmarking of new functionals

Karim Bennaceur	IPN Lyon & Jyväskylä
Dany Davesne	IPN Lyon
Robin Jodon	IPN Lyon
Jacques Meyer	IPN Lyon
Alessandro Pastore	formerly IPN Lyon, now University of York
Jeremy Sadoudi	Irfu/CEA Saclay first, then CEN Bordeaux Gradignan

color code: active (past) member of the collaboration